Full Length Article

Cytotoxic potential of Commicarpus plumbagineus extracts against liver cancer cell lines through In-Vitro and In-Silico methods

Raed Alghamdi, Nael Abutaha, Muhammad Al- Wadaan [*]

Department Zoology, College of Science, King Saud University, P.O. Box 2455, Riyadh 11451, Saudi Arabia

ABSTRACT

Hepatocellular carcinoma holds the fifth position in terms of worldwide cancer prevalence. The challenges posed by drug adverse effects and resistance associated with existing anticancer therapies underscore the importance of exploring natural sources for potential solutions. This study assessed the in-vitro cytotoxicity of a range of solvent extracts (n-hexane, ethyl acetate, and methanol) against liver cancer cell lines using (3-(4,5-Dimethylthiazol-2-yl)-2,5-Diphenyltetrazolium Bromide) (MTT) assay. The bioactive extract was also examined for its impact on cell migration and subjected to in-silico predictions targeting 14 different protein targets. The results indicated that only the ethyl acetate (F2) extract was cytotoxic. The IC_{50} values for the F2 were 300, 320 and 318 µg/mL against HepG2, HuH7, and normal HUVECs cell lines, respectively. A significant reduction in the % relative migration of cells following treatment with 87.5 µg/mL of F2 extract was observed. The apoptotic potential of F2 was seen on HepG2 cells using the DAPI and AO/EtBr staining. The F2 extract underwent GC–MS analysis, uncovering the existence of 23 phytocompounds, which were subsequently employed in molecular docking studies. Loperamide, á-Sitosterol, and stigmasterol exhibited the highest binding affinity (−10.90 kcal/mol) for 4WEV and 4NOS. These phytochemicals from the F2 extract hold potential as promising drug candidates for liver cancer, subject to further validation.

1. Introduction

Liver cancer is an aggressive cancer with a significant global fatality rate (Organization, 2020). Hepatocellular carcinoma stands as the most frequently occurring form of primary liver cancer, while cholangiocarcinoma represents the remaining cases (Xu et al., 2018). Despite conventional treatments such as chemotherapy and surgical resection, the prognosis for liver cancer patients remains unfavourable. Despite notable progress in cancer treatment strategies, the occurrence of adverse effects and the development of resistance to currently available anticancer medications remain major factors contributing to treatment failure in approximately 80 % of patients (Khamis et al., 2018). While chemotherapeutic agents have shown high efficacy in treating breast cancer, prolonged use is often necessary to achieve optimal outcomes. The current targeted therapy for breast cancer includes medications like Herceptin, fulvestrant, tamoxifen, and aromatase inhibitors. Nonetheless, the development of resistance to chemotherapeutic drugs presents a substantial obstacle (Lukong, 2017). Furthermore, in addition to their cancer-fighting properties, chemotherapeutic drugs can lead to severe

health conditions, including endometrial and ovarian hyperplasia, carcinomas, and the development of pulmonary embolism and multiple vein thrombosis (Davies et al., 2013). Although these agents effectively target and eliminate malignant cells, they can also damage healthy cells and tissues, ultimately diminishing the overall life expectancy of patient (Talib et al., 2021). As a result, researchers are exploring alternative therapeutic approaches, including the use of traditional plant extracts. The search for innovative, targeted, safe, cost-effective therapeutic approaches has become crucial. Medicinal plants offer a promising avenue as they are relatively safe and affordable, making them attractive candidates for developing potential new anticancer compounds (Bournine et al., 2017). Natural products and phytomedicines are promising to treat cancer and various other diseases. Several plant-derived compounds, such as Vincristine,Taxol, Vinflunine, Vindesine, Camptothecin, Vinorelbine, Vinblastine, and others, have demonstrated significant therapeutic value in the treatment of cancers (Greenwell and Rahman., 2015). Plant extracts have been the subject of several studies, and their anticancer properties, including their ability to bring apoptosis in liver cancer cells, have been documented (Kim et al., 2023) (Suknoppakit

Fig. 1. Flowers of *Commicarpus plumbagineus* Standl. (Nyctaginaceae) collected from Taif, Saudi Arabia.
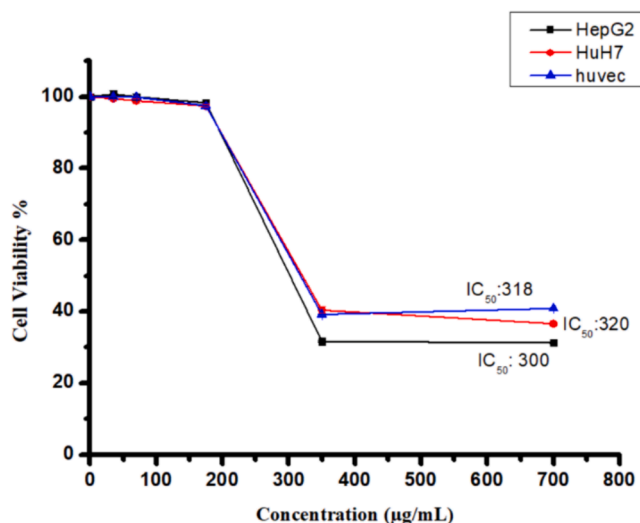

Fig. 2. The cytotoxicity of the F2 extract from *C. plumbagineus* was evaluated on human liver cancer cells (HepG2 and HuH7) and non-cancerous cells (Huvec) using various concentrations (0–700 μg/mL) for a 24-hour treatment. Cell viability was assessed through the MTT assay, and statistical analysis was carried out utilising Student's *t*-test. The data, presented as the mean ± standard deviation, were derived from three replicates. Significance was established at *p < 0.05 in comparison to the control group.

et al., 2023).

Commicarpus plumbagineus, belonging to the Nyctaginaceae family, is present diverse geographical areas, encompassing Africa, India, Palestine, Jordan, and the Arabian Peninsula. In Saudi Arabia, mainly in the Asir and Taif, it is commonly known as 'Roqma.' Traditional Saudi Arabian medicine has long utilised the plant's leaves to address ailments such as asthma (Qari et al., 2021). Additionally, it is employed for jaundice treatment, as a laxative, expectorant, and for managing swollen glands, burns, and ulcers.

The study aimed to explore a natural remedy for hepatocellular carcinoma. Considering the preceding context, *C. plumbagineus* extracts have not yet been explored for their anticancer potential. Furthermore, investigations involving cell migration assay, apoptosis assessment via fluorescence microscopy, chemical profiling via Gas Chromatography-Mass Spectrometry (GC–MS), and in silico studies to predict mechanisms of action are warranted.

2. Material and method

2.1. Collection of plant material

The aerial part (flower, stem and leaf) of *Commicarpus plumbagineus* (Fig. 1) was collected from Taif (21°14′11.4″N 40°25′16.5″ E), Saudi Arabia. The voucher specimen (KSU-T042) was placed at the Bio-product Research Chair, King Saud University.

2.2. Preparation of plant extracts

After harvesting, the aerial parts were cleaned using distilled water, air-dried, finely powdered, and stored in sealed plastic bags at a temperature of −20 °C. Different extraction techniques were applied, and the extraction yield was calculated using the provided formula:

Extraction yield (%) = (weight of dry extracted material (g)/weight of fine powder (g)) × 100.

2.3. Soxhlet extraction

The Soxhlet system was employed for the extraction process. A 15-gram sample of air-dried powdered *C. plumbagineus* was placed within a thimble holder and subsequently subjected to sequential extraction using n-hexane (F1), ethyl acetate (F2), and methanol (F3) solvents (450 mL each). The extraction was conducted for 24 h at 60 °C. The extraction process was considered complete when the solution in the thimble became clear, indicating complete extraction of the dried powder. Subsequently, the extracts were rotary evaporated at a vacuum and a temperature of 45 °C. The resulting extracts were preserved (−20 °C) for future use.

2.4. Maceration method

A quantity of 50 g of the plant powder was soaked in a closed flask containing 70 % methanol. The mixture underwent sonication (Wise-Clean, Korea) for 10 min while intermittently shaken over 5 days. Afterwards, the mixture was filtered. The solvent from the resulting filtrate (Whatman filter paper No.1, UK) was rotary evaporated (Heidolph, Germany) at a vacuum and a temperature of 40 °C. The resulting dry crude extract was subsequently reconstituted in distilled water and subjected to liquid–liquid extraction using n-hexane (F4) (3x 100 mL), ethyl acetate (F5) (3x 100 mL), and n-butanol (F6) (3x 100 mL). The resulting extracts were preserved (−20 °C) for future use.

2.5. Saponin extraction

To extract the desired compounds, 30 g of the powder was soaked in a closed flask containing 500 mL of 20 % ethanol. The mixture underwent sonication for 10 min with intermittent shaking. The flask was placed in a water bath (55 °C) for 4 h. To remove any solid particles, the extract was filtered through a glass funnel with two layers of cheesecloth. Further purification was achieved by centrifuging the extract for three minutes at 4000 rpm. The concentrated extract was obtained using a vacuum rotary evaporator (Heidolph, Germany) at a temperature of 45 °C until the volume was reduced to 200 mL. To eliminate fats and lipids, the extract was subjected to defatting using hexane in three successive extractions (each with 200 mL of hexane). Subsequently, the extract was further processed thrice with n-butanol (F7) (each with 200 mL) using a separatory funnel. The resulting n-butanol extract (F7) was then evaporated and stored at −20 °C for future use.

2.6. Cell lines

Human hepatocellular carcinoma cells HuH7 and HepG2 and human umbilical vein endothelial non-cancerous cell line (HUVECs) (DSMZ, Germany) were maintained in DMEM (Gibco) supplemented with fetal
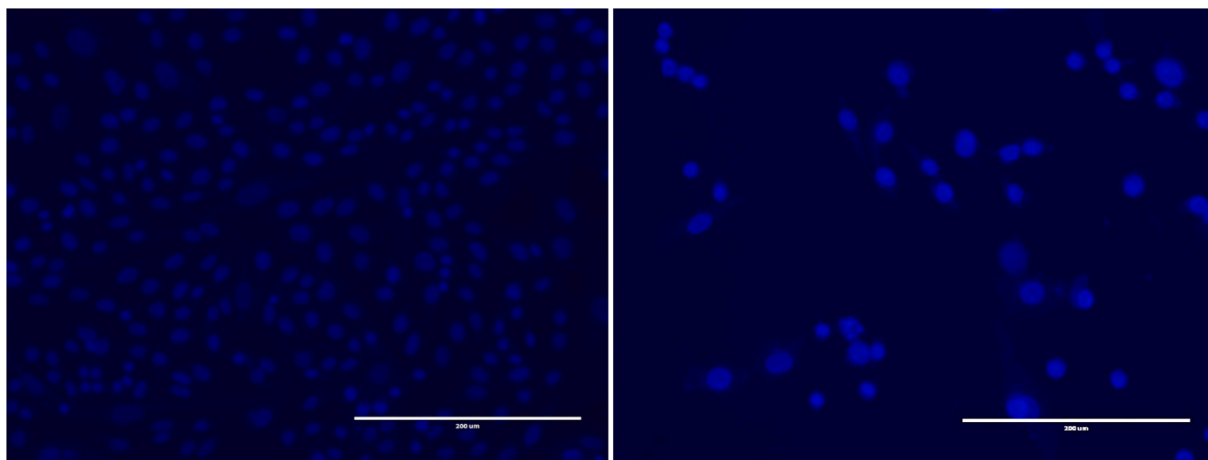
Fig. 3. Fluorescent photomicrographs depict the HepG2 cancer cell line stained with DAPI after exposure to the F2 extract (300 µg/mL). The panels illustrate the following: (A) Untreated HepG2 cell line, (B) Treated HepG2 cell line after 24 h of incubation.

bovine serum (FBS 10 %) (Gibco), 10 mM L-glutamine, at 37 °C in CO_2 incubator. Cells were harvested with trypsin/EDTA (Gibco), washed with the media, and then used (Al-Zharani and Abutaha, 2023).

2.7. In vitro cytotoxic activity

HuH7, HepG2, and HUVECs cells (50,000 cells/mL) were collected, washed with DMEM medium, and then seeded into 24-well cell tissue culture plates. The plates were placed in a CO_2-humidified incubator for 24 h. The cells were treated with 700, 350, 175, 70, and 35 µg/mL of extract. The methanol concentration remained below 0.05 %, a dosage that does not affect cell viability. Cell viability assays were performed in triplicate to evaluate the impact of the plant extracts. The MTT assay was employed to assess the viability of cell. In this assay, cells were incubated with the MTT, which is reduced by viable cells to form a formazan product. After a 48-hour treatment period, the MTT solution was pipetted. After an additional 2-hour incubation period, the MTT reagent was withdrawn, and the formed formazan crystals were dissolved by introducing 0.01 % acidified methanol. It is quantified using a plate reader (540 nm), and the results were recorded as a percentage of control (Al-Zharani and Abutaha, 2023).

2.8. Cell migration assay

HepG2 cells were cultured in 6-well cell tissue culture plates until a monolayer is formed. Once they reached a confluence of 70 %, a scratch was created by gently scratching the cell surface using a 200 µL Pipette tip, making horizontal lines and removing the cell debris. The cells were then incubated at 300 µg/mL to investigate its impact on cell migration. After 24 h, images were taken using a Leica microscope (Leica, Germany). The images were analysed using ImageJ software (NIH, USA). The calculation of the relative cell migration was performed using the following formula:

$$\text{Relative Migration Ratio} = \left(\frac{\text{Distance at 0 h} - \text{Distance at 24 h}}{\text{Distance at 0 h}} \right)$$

2.9. Cell morphology assessment

In 24-well plates, 50,000 cells were cultured per well and exposed to 300 µg/mL of the extract for a 24-hour. Following this treatment, we observed morphological changes using an inverted phase contrast microscope (Leica, Germany).

2.10. Apoptosis assessment by fluorescence microscopy

The test followed the previously described method (Alsayadi et al., 2022). In brief, Post 48 h of treatment, the cells were fixed with ice-cold ethanol for 5 min. Subsequently, 1 µl of 4′,6-diamidino-2-phenyl indole (DAPI, 1 mg/mL) was pipetted to each well. Post a 5-minute of dark incubation (25 °C), the cells were rinsed with PBS (pH 7.2).

Acridine orange and ethidium bromide (AO/EtBr) duel staining method was utilised to differentiate live and apoptotic cells following the procedure outlined in reference (Alsayadi et al., 2022). To summarise, treated and untreated cells were evaluated using a fluorescence microscope with excitation wavelengths of 488 nm and 550 nm. The fluorescently stained cells were visualised using EVOS fluorescent microscope (USA).

2.11. Gas Chromatography-Mass spectroscopy (GC–MS)

GC–MS analysis was conducted using a GC-TSQ mass spectrometer (Thermo Scientific, USA). One microliter of the extract was introduced into the TG–5MS capillary column (30 m x 0.25 mm x 0.25 µm). The temperature protocol began at 60 °C and was gradually elevated to 250 °C at a rate of 5 °C per minute, followed by a 2-minute hold, and then increased to 300 °C at a rate of 30 °C per minute. The injector maintained a temperature of 270 °C. Helium was employed as the carrier gas with a constant flow rate of 1 ml/min. Compound identification was accomplished by comparing their mass spectra to those in the WILEY 09 and NIST14 mass spectral databases (Abd El-Kareem et al., 2016).

2.12. In silico studies

The ligand molecules' three-dimensional (3-D) structures were downloaded in sdf format (https://pubchem.ncbi.nlm.nih.gov/) and converted into pdb format structures using https://openbabel.org. The ligands underwent optimisation by adding Gasteiger charges and hydrogen atoms. Ligand structures in pdbqt format were then generated using AutoDock Tools 1.5.7 (Morris et al., 2009). These prepared ligand structures were used as input for the docking simulation, which was assessed using AutoDock Vina (https://vina.scripps.edu/).

The x-ray crystallography structure of protein molecules (1RWB, 2AZ5, 4LVT, 4MAN, 4MAN2, 4NOS, 4RT7, 4XUF, 6CJE, 6JQR, 6O0K, 6CJE, 6JQR, 6O0K, 6O6F, 1 M17, 1SVC, 2AR9, 4ASD, 2BMC, 2O2F, 4C61, 4WEV, 5KIR, 4C61, 4XCU, and 4X13) were obtained from https://www.rcsb.org. The receptors were prepared by excluding water molecules and incorporating polar hydrogen atoms and Kollman
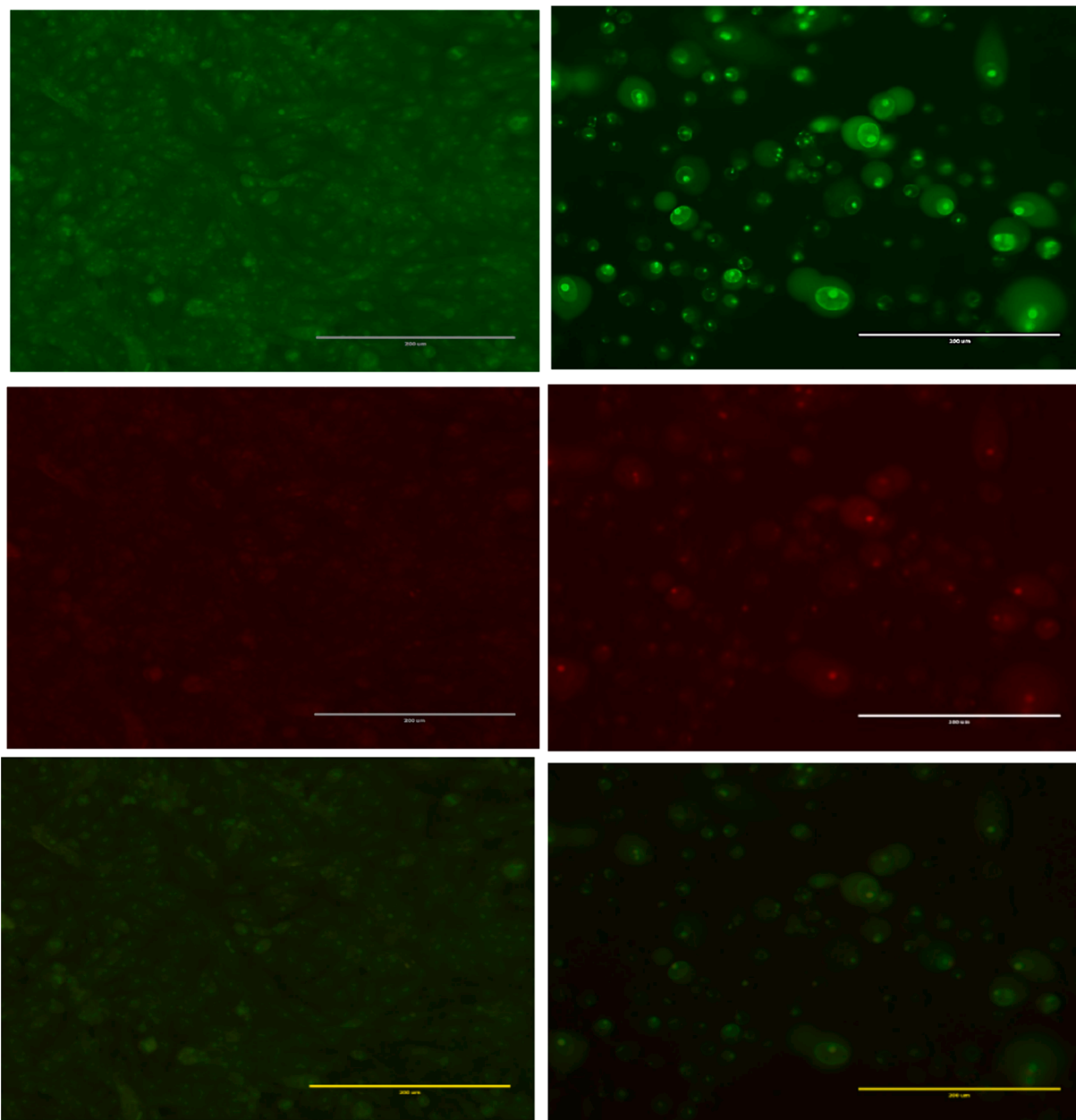
Fig. 4. Acridine orange/ethidium bromide staining of HepG2 cells to detect apoptosis induced by F2 extract from *C. plumbagineus* (300 μg/mL). (A) negative control (B) treated cells. Live cells are uniformly green (L). In contrast, apoptotic cells (AP) are characterised by green and fragmented chromatin.

charges. AutoDock Tools 1.5.7 was employed to generate the pdbqt format for the receptors. Following this, AutoDock Vina was executed on the Windows 10.0 operating system to perform the docking simulations. (Van et al., 2022). The binding between the target proteins and ligands was visually analysed using Discovery Studio 2021.

3. Result

3.1. Extraction and yield calculation of C. plumbagineus extracts

The dry extract yield of the aerial part of C. plumbagineus obtained through the Soxhlet extraction method was 2.66 %, 0.26 %, and 1.08 % for the hexane (F1), ethyl acetate (F2), and methanol (F3) extracts, respectively. Additionally, a 70 % methanol extraction of 50 g of C. plumbagineus followed by liquid–liquid partitioning yielded the n-hexane fraction (F4) (17.5 % yield), ethyl acetate (F5) fraction (1.2 % yield), and n-butanol (F6) fraction (68.4 % yield). To extract saponin (F7), 50 g of dry samples were extracted with 20 % ethanol, resulting in a dry extract yield of 27.7 %.

3.2. Cytotoxicity potential

The cytotoxic properties of seven different extracts of *C. plumbagineus* were evaluated across HuH7, HepG2, and HUVECs cell lines using the MTT assay at concentrations ranging from 0 to 700 μg/mL. The results revealed that increasing the concentration of the ethyl acetate extract (F2) resulted in a notable reduction in viable cell count, indicating enhanced cytotoxicity compared to control-treated cells (Fig. 2). Conversely, the other extracts (F1, F3, F4, F5, F6, and F7) exhibited no significant cytotoxicity at the highest tested concentration of 700 μg/ mL. Furthermore, the determination of IC_{50} values for the F2 extract indicated its potency against the respective cell lines. Specifically, the IC_{50} values for the F2 extract were determined to be 300 μg/mL, 320 μg/ mL, and 318 μg/mL against HepG2, HuH7, and HUVECs cell lines, respectively. These findings underscore the cytotoxicity of the F2 extract
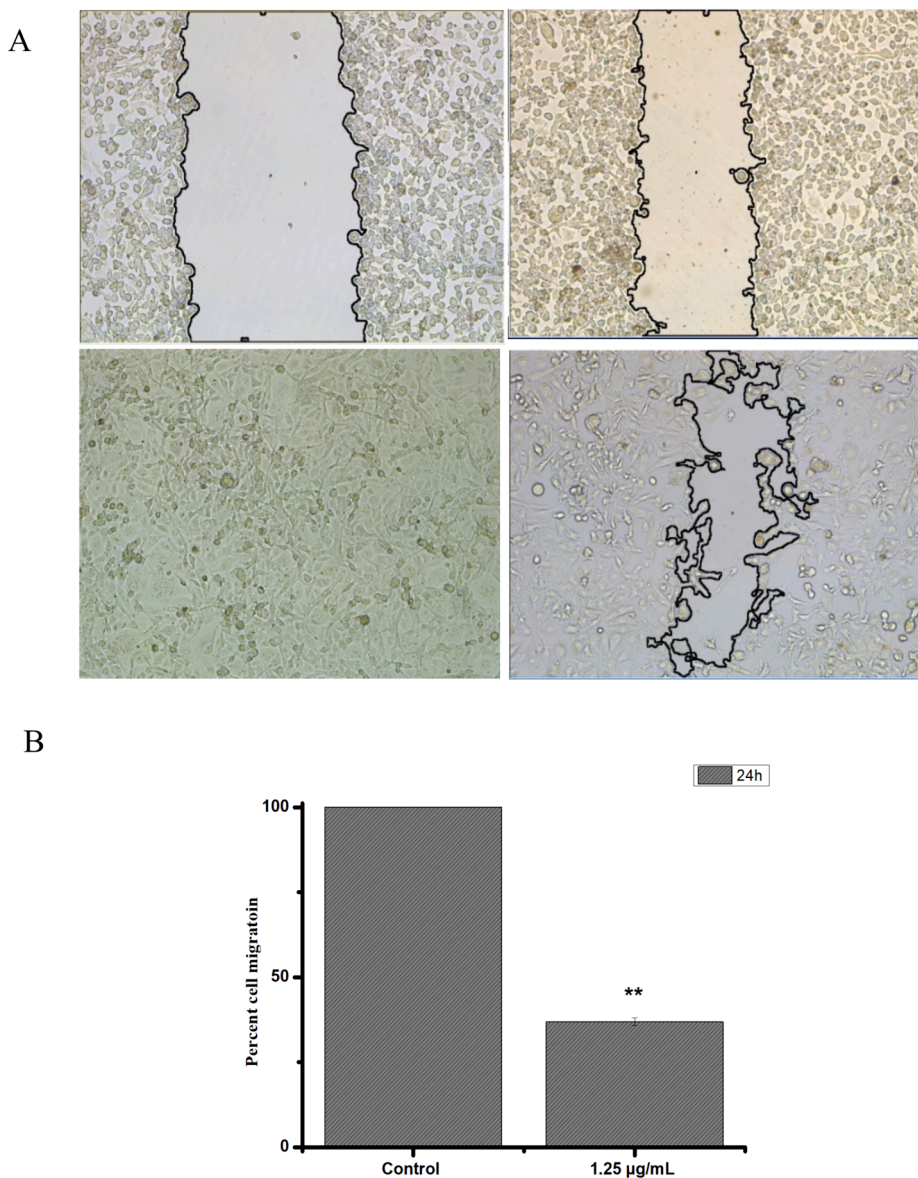
Fig. 5. The effects of the F2 extract from *C. plumbagineus* on the migration of HepG2 cells were evaluated. Figure A displays images of the wound monolayer of HepG2 cells at two points: immediately after wounding (t = 0 h) and after a 24-hour incubation period. Cells were either left untreated (control) or treated with the extract at 87.5 µg/mL. Figure B illustrates the calculated cell migration rate using the methodology described in the materials and methods section. The experiments were performed in triplicate, and statistical analysis was conducted using Student's *t*-test (*p < 0.05 vs control).

and its potential as a therapeutic agent. **Assessment of cell nuclear morphology using fluorescent microscopy**.

The results demonstrated a higher number of cells with fragmented and condensed nuclei in the HepG2 cell population after exposure (24 h) to the F2 extract (300 µg/mL) compared to normal cells (control). Fig. 2 presents fluorescent photomicrographs of DAPI-stained cancer cells, revealing that the treated cell lines exhibited apoptosis characteristics, including the formation of apoptotic bodies, nucleus fragmentation, cell shrinkage and membrane blebbing. In contrast, as shown in Fig. 3, untreated cells did not display these distinctive apoptotic features.

To verify the apoptotic effects of the extract, the cells were stained with AO/ EtBr.This staining method allowed us to observe distinct morphological changes in the treated cancer cells, indicative of apoptosis. Viable cells appeared green under the microscope, as they were stained solely with AO. Furthermore, early apoptotic cells, which displayed green and orange fluorescence, showed condensed chromatin, as evidenced by staining with AO and EtBr. The results obtained from HepG2 cells treated with the extract indicated that apoptosis was the predominant mode of cell death, as marked by chromatin condensation and loss of membrane integrity (Fig. 4). Therefore, the microscopic analysis suggests that the extract likely triggered apoptosis in HepG2 cells.

3.3. Inhibition of HepG2 cells migration by F2 extract

To evaluate the impact of putative inhibitors on cell migration, we employed a wound healing assay, where a mechanical scratch was created, and the cells' migratory response was observed. Images of the scratch areas at 0 and 24 h were captured and presented in Fig. 5. The control group demonstrated complete scratch closure after 24 h, serving as a representative example. To quantify the effects of the migration inhibitors, we determined the percentage of the remaining open wound area after 24 h, as shown in Fig. 5 A and B. Our findings demonstrate that treatment with the extract significantly impeded cell migration, as evidenced by the decrease in the percentage of the open wound area after 24 h.

Table 1

Phytoconstituents detected in the ethyl acetate extract (F2) from *Commicarpus plumbagineus* using gas chromatography-mass spectrometry.

| No.	Retention Time	Name of the Compound	Area %	Molecular Formula	Molecular Weight
1	24.17	Z,Z-3,15-Octadecadien-1-ol acetate	0.45	$C_{20}H_{36}O_2$	308
2	25.64	Pentadecanoic acid	0.85	$C_{17}H_{34}O_2$	270
3	26.46	Hexadecanoic acid	14.28	$C_{16}H_{32}O_2$	256
4	28.64	9,12-Octadecadienoic acid (Z,Z)-, methyl ester	3.56	$C_{19}H_{34}O_2$	294
5	28.83	11-Octadecenoic acid, methyl ester	3.64	$C_{19}H_{36}O_2$	296
6	28.93	10-Octadecenoic acid, methyl ester	0.77	$C_{19}H_{36}O_2$	296
7	29.15	Phytol	6.20	$C_{20}H_{40}O$	296
8	29.50	9,12-Octadecadienoic acid (Z,Z)-	21.48	$C_{18}H_{32}O_2$	280
9	29.63	*trans*-13-Octadecenoic acid	18.63	$C_{18}H_{34}O_2$	282
10	30.10	9-Octadecenoic acid (Z)-	1.73	$C_{18}H_{34}O_2$	282
11	31.34	Glycidyl oleate	0.40	$C_{21}H_{38}O_3$	338
12	34.02	9,12,15-Octadecatrienoic acid, 2,3-dihydroxypropyl ester, (Z,Z,Z)-	1.68	$C_{21}H_{36}O_4$	352
13	34.78	*cis*-5,8,11,14,17-Eicosapentaenoic acid	0.78	$C_{20}H_{30}O_2$	302
14	35.82	Diisooctyl phthalate	5.93	$C_{24}H_{38}O_4$	390
15	39.02	1,3-Benzenedicarboxylic acid, bis(2-ethylhexyl) ester	3.13	$C_{24}H_{38}O_4$	390
16	42.19	Loperamide	1.00	$C_{29}H_{33}ClN_2O_2$	476
17	42.55	9,12-OCTADECADIENOIC ACID (Z,Z)-,	1.20	$C_{27}H_{54}O_4Si_2$	498
18	42.67	ARABINITOL, PENTAACETATE	0.68	$C_{15}H_{22}O_{10}$	362
19	42.96	2-Methyl-E,E-3,13-octadecadien-1-ol	0.75	$C_{19}H_{36}O$	280
20	43.93	Campesterol	2.08	$C_{28}H_{48}O$	400
21	44.23	1-Heptatriacotanol	1.29	$C_{37}H_{76}O$	536
22	44.75	á-Sitosterol	5.94	$C_{29}H_{50}O$	414
23	44.88	Stigmasterol	3.57	$C_{29}H_{48}O$	412
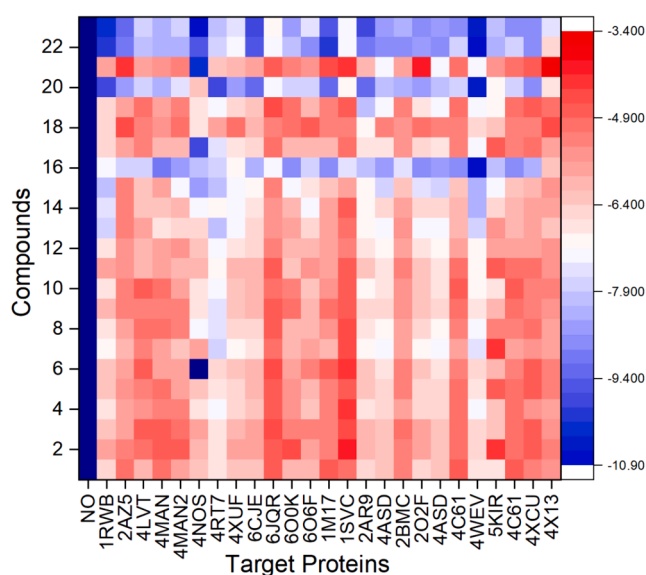
Fig. 6. Heatmap of molecular docking scores of ligands numbered from 1 to 23 as reported in Table 1 and target proteins.

3.4. Molecular docking analysis for liver cancer inhibitors

Various compounds were subjected to docking against 14 different target proteins, and only those compounds demonstrating high binding affinities (equal to or greater than 10.0 kcal/mol) with these target proteins were selected for further analysis. This suggests their potential for advancement as potential anticancer drugs, as detailed in Table 1. Specifically, stigmasterol, β-Sitosterol, campesterol, 1-heptatriacotanol, and loperamide exhibited strong binding affinities with four target proteins, namely 1RWB, 4NOS, 1 M17, and 4WEV. Loperamide, á-sitosterol, and stigmasterol demonstrated the most robust binding affinity (−10.90 kcal/mol) for 4WEV and 4NOS. The docking of loperamide on 4WEV showed 8 hydrophobic interactions with 7 residues namely TRP21, LYS22, TYR210 (2x), LEU213, PRO216, ASP217, and ILE261. The docking of á-sitosterol on 4WEV shows 5 hydrophobic interactions with 4 residues: PHE 4 (4x), GLU6, ASP72, PHE74 and one

hydrogen bond with LEU73. Stigmasterol was bound to 4NOS protein with a binding affinity of − 10.9 kcal/ mol. It formed multiple hydrophobic interactions with 4NOS with 9 residues TRP194, ALA197, ARG199, ILE201, GLN205, VAL352, TRP372, and TYR489 (2x) and one hydrogen bond with TYR489.

4. Discussion

Liver cancer is acknowledged as an aggressive type of cancer, presenting substantial challenges because of its progression risk and poor prognosis. The absence of successful targeted treatments further exacerbates the complexities in addressing this disease (Anwanwan et al., 2020). Challenges such as side effects, toxicity, non-targeted effects, psychological impact, long-term consequences, cost, limited effectiveness, resistance, and complex dosing regimens pose significant hurdles during long-term conventional cancer therapies (Anwanwan et al., 2020) (Pearce et al., 2017). Consequently, current research is increasingly centred on discovering alternative natural treatment approaches with reduced or minimal adverse effects.

Numerous research studies have unveiled the potential anticancer properties of medicinal plants, which contain various therapeutic natural compounds. These medicinal constituents exert their effects through diverse mechanisms against tumours, with a common involvement in inducing apoptosis (Greenwell and Rahman, 2015) (Bhosale et al., 2020) (Safarzadeh et al., 2014). Apoptotic induction is a crucial aspect in the search for anticancer agents, as dysregulation of apoptosis is closely linked to cancer (Choi et al., 2008) (Lu et al., 2011).

Different studies have revealed the cytotoxic effects of various members of the Nyctaginaceae family against different types of cancers. For instance, Sinan et al. demonstrated that both aqueous and methanol extracts of *Boerhavia diffusa* exhibited cytotoxic properties in the MDA-MB-231 cell line (Sinan et al., 2021). Likewise, Shareef et al. reported the cytotoxic potential of *Boerhavia erecta* extract against human brain tumour cell lines (U87) (Shareef et al., 2017).

There is limited available data regarding the cytotoxic effects of the *C. plumbagineus* extract on cancer cells. Our investigation observed the cytotoxicity and apoptotic effects of the *C. plumbagineus* F2 extract on liver cancer cells in a concentration-dependent mode. This was assessed through various methods, including an MTT assay (Fig. 2) and DAPI and AO/EtBr staining (Figs. 3 and 4).

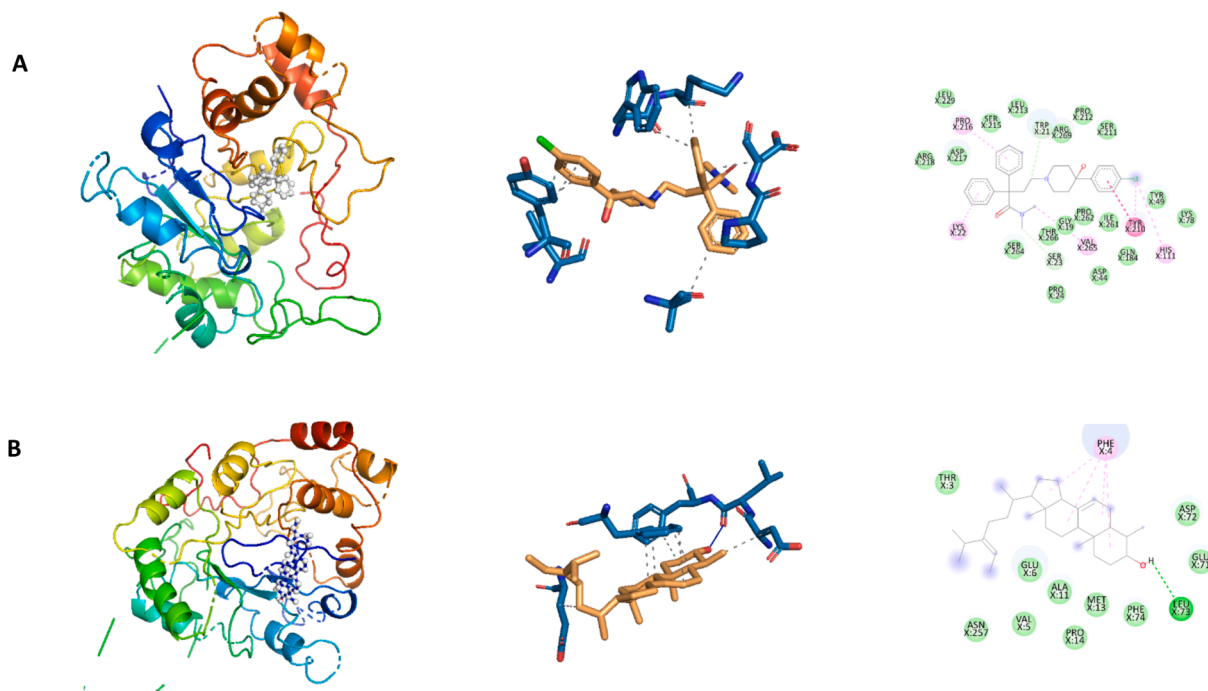Regarding the HepG2 cell migration, it's important to highlight that

Fig. 7. The docked poses of compounds and 3D structures of docked complexes of secondary metabolites, (A) Loperamide (−10.90 kcal/mol) and (B) á-Sitosterol (−10.90 kcal/mol) in the substrate binding sites of 4WEV.
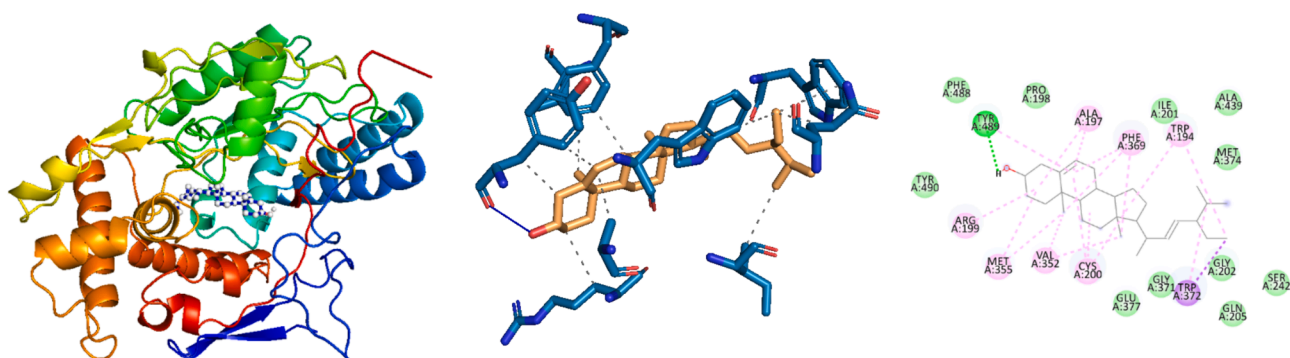

Fig. 8. The docked pose and 3D structure of the docked complex of stigmasterol in the substrate binding sites of 4NOS (10.90 kcal/mol).

the F2 extract demonstrated a notable suppressive effect on the migration of HepG2 cells, reducing their invasiveness by 28.2 %. In vivo and in vitro investigations have provided evidence that secondary metabolites derived from *Salvia miltiorrhiza* exhibit repressing impacts on the migration of diverse cancer cells, including osteosarcoma cells, as demonstrated in different studies (Zhang et al., 2012) (Xie et al., 2020). Similarly, the topical application of methanol extract (ME) from *Boerhavia diffusa* leaf, a member of the Nyctaginaceae family, significantly reduced the wound area in an excision wound model by the 14th day. Specifically, the reduction in wound area was 91 %, compared to 22 % in the control group (Juneja et al., 2020).

The F2 extract was selected for GC–MS analysis due to its enhanced anticancer potential. The analysis revealed the existence of bioactive metabolites in the F2 extract (Table 1). Notably, 9,12-Octadecadienoic acid (Z,Z)- exhibited the highest peak area percentage and has previously been identified in many plants, known for its antimicrobial properties (Rahman et al., 2014; Wei et al., 2011). This compound has also exhibited analgesic, anti-inflammatory and ulcerogenic properties (Hadi et al., 2016). An additional compound, ethyl ester of 9,12-Octadecadienoic acid (a fatty acid ester), is recognised for its antimicrobial and hepatoprotective properties. (Adeoye-Isijola et al., 2018). Similarly,

hexadecanoic acid is also reported for its antioxidant, antiandrogenic, hypocholesterolemic, lubricant, and 5-Alpha reductase inhibitor (Rajeswari et al., 2012).

In drug discovery, the utilisation of bioinformatic tools has become prevalent for the prediction of drug-like bioactive molecules. These computational methodologies are extensively employed to forecast the therapeutic properties of secondary metabolites, which are subsequently confirmed through in-vivo and in-vitro studies (Ekins et al., 2007).

In this study, we have selected a specific set of protein targets (1RWB, 2AZ5, 4LVT, 4MAN, 4MAN2, 4NOS, 4RT7, 4XUF, 6CJE, 6JQR, 6O0K, 6CJE, 6JQR, 6O0K, 6O6F, 1 M17, 1SVC, 2AR9, 4ASD, 2BMC, 2O2F, 4C61, 4WEV, 5KIR, 4C61, 4XCU, and 4X13) due to their significant roles in liver and other carcinogenesis. Only stigmasterol, β-sitosterol, campesterol, 1-heptatriacotanol, and loperamide among the twenty-three bioactive molecules under investigation exhibited promising results, with higher docking scores against 1RWB, 4NOS, 1 M17 and 4WEV protein targets (Figs. 6 and 7).Fig. 8.

Aldose reductase (AR) enzymes play crucial roles in significant pathologies, including diabetes and cancer, making them attractive targets for drug development. Numerous studies have indicated that aldose reductase (AR) is upregulated in various pathological conditions

associated with oxidative stress and inflammation, including restenosis, vascular inflammation, myocardial ischemia, heart failure, alcoholic liver cirrhosis and cancer (Tammali et al., 2011). In the present investigation, loperamide, á-sitosterol, and stigmasterol demonstrated the most robust binding affinity (−10.90 kcal/mol) for 4WEV.

Receptor tyrosine kinases, including insulin receptor (IR), insulin-like growth factor 1 receptor (IGF1R), epidermal growth factor receptor (EGFR), and vascular endothelial growth factor receptor (VEGF2) are recognised for their role in regulating various biological processes such as apoptosis and cellular growth (Singh et al., 2014). Researchers have increasingly focused on these receptors as promising targets for cancer treatment due to ample evidence indicating their overexpression on cancer cells. Numerous studies have demonstrated that green tea can be cytotoxic and induce apoptosis in cancer cell lines, including Ishikawa cells, prostate, colorectal and liver cancer cells and SV40 virally transformed cells (Li et al., 2014) (Raffoul et al., 2012). In the present study, the interaction between á-Sitosterol and EGFR (PDB ID: 1 M17) exhibited a noteworthy binding affinity of −10.10 kcal/mol.

Inducible nitric oxide synthase (iNOS) plays a crucial role in inflammatory processes (Kim et al., 2005). The production of NO through iNOS activity is a key driver of inflammation and has been implicated in numerous diseases, such as cancer (Bian and Murad, 2003). Additionally, iNOS has been associated with activating another major inflammatory mediator, cyclooxygenase-2 (COX-2) (Kim et al., 2005). Consequently, there is a strong need to develop iNOS inhibitors and research efforts have been directed toward natural products as potential sources for discovering such inhibitors (Murakami and Ohigashi, 2007).

Researchers noticed that iNOS inhibitors effectively inhibited cell proliferation in the PDX human model of HCC24. Another study demonstrated that *Nigella sativa*'s anti-carcinoma effect was achieved by reducing the activity of the iNOS pathway and mitigating the inflammatory response mediated by TNF-α in HCC25 (Fathy and Nikaido, 2013). In the current study, the interactions between 1-Heptatriacotanol and stigmasterol with iNOS (PDB ID: 4NOS) demonstrated notable binding affinities of −10.30 kcal/mol and 10.9 kcal/mol, respectively.

As such, these compounds represent strong candidates for inclusion in various anticancer therapeutic strategies against Hepatocellular Carcinoma (HCC). Nonetheless, conducting more comprehensive in vivo investigations to substantiate their effectiveness and ensure their safety profiles before considering their use in clinical applications is imperative.

5. Conclusion

This study is important because it explores natural compounds as potential treatments for HCC. The treatment with F2 extract showed cytotoxicity and triggered apoptosis. These results suggest that the F2 extract could serve as a potential supplementary treatment for liver cancer. Additional research is necessary to pinpoint the active compounds and clarify their modes of action, which would enhance our comprehension of their therapeutic efficacy. Subsequent validation and clinical trials will be essential to validate their therapeutic potential in the future.

6. Research funding

Declaration of Competing Interest

The authors declare that they have no known competing financial interests or personal relationships that could have appeared to influence the work reported in this paper.

References

M.S. Abd El-Kareem M.A.E.F. Rabbih E.T.M. Selim Elsherbiny, E.A.E.-m., El-Khateeb, A.Y. Application of GC/EIMS in combination with semi-empirical calculations for identification and investigation of some volatile components in basil essential oil International Journal of Analytical Mass Spectrometry and Chromatography 4 1 2016 14 25.

Adeoye-Isijola, M.O., Olajuyigbe, O.O., Jonathan, S.G., Coopoosamy, R.M., 2018. Bioactive compounds in ethanol extract of Lentinus squarrosulus Mont-a Nigerian medicinal macrofungus. African Journal of Traditional, Complementary and Alternative Medicines 15 (2), 42–50.

Alsayadi, A.I., Abutaha, N., Almutairi, B.O., Al-Mekhlafi, F.A., Wadaan, M.A., 2022. Evaluating the efficacy of an innovative herbal formulation (HF6) on different human cancer cell lines. Environ. Sci. Pollut. Res. 29 (34), 51768–51777.

Al-Zharani, M., Abutaha, N., 2023. Phytochemical screening and GC-MS chemical profiling of an innovative herbal formula (PHF6). Journal of King Saud University-Science 35 (2), 102525.

Anwanwan, D., Singh, S.K., Singh, S., Saikam, V., Singh, R., 2020. Challenges in liver cancer and possible treatment approaches. Biochimica et Biophysica Acta (BBA)-Reviews on. Cancer 1873 (1), 188314.

Bhosale, P.B., Ha, S.E., Vetrivel, P., Kim, H.H., Kim, S.M., Kim, G.S., 2020. Functions of polyphenols and its anticancer properties in biomedical research: a narrative review. Transl. Cancer Res. 9 (12), 7619.

Bian, K., Murad, F., 2003. Nitric oxide (NO)–biogeneration, regulation, and relevance to human diseases. Frontiers in Bioscience-Landmark 8 (4), 264–278.

Bournine, L., Bensalem, S., Fatmi, S., Bedjou, F., Mathieu, V., Iguer-Ouada, M., Kiss, R., Duez, P., 2017. Evaluation of the cytotoxic and cytostatic activities of alkaloid extracts from different parts of Peganum harmala L. (Zygophyllaceae). European Journal of Integrative Medicine 9, 91–96.

Choi, B.-H., Kim, W., Wang, Q.C., Kim, D.-C., Tan, S.N., Yong, J.W.H., Kim, K.-T., Yoon, H.S., 2008. Kinetin riboside preferentially induces apoptosis by modulating Bcl-2 family proteins and caspase-3 in cancer cells. Cancer Lett. 261 (1), 37–45.

Davies, C., Pan, H., Godwin, J., Gray, R., Arriagada, R., Raina, V., Abraham, M., Alencar, V.H.M., Badran, A., Bonfill, X., 2013. Long-term effects of continuing adjuvant tamoxifen to 10 years versus stopping at 5 years after diagnosis of oestrogen receptor-positive breast cancer: ATLAS, a randomised trial. Lancet 381 (9869), 805–816.

Ekins, S., Mestres, J., Testa, B., 2007. In silico pharmacology for drug discovery: applications to targets and beyond. Br. J. Pharmacol. 152 (1), 21–37.

Fathy, M., Nikaido, T., 2013. In vivo modulation of iNOS pathway in hepatocellular carcinoma by Nigella sativa. Environ. Health Prev. Med. 18, 377–385.

Greenwell, M., Rahman, P., 2015. Medicinal plants: their use in anticancer treatment. Int. J. Pharm. Sci. Res. 6 (10), 4103.

Hadi, M.Y., Mohammed, G.J., Hameed, I.H., 2016. Analysis of bioactive chemical compounds of Nigella sativa using gas chromatography-mass spectrometry. Journal of Pharmacognosy and Phytotherapy 8 (2), 8–24.

Juneja, K., Mishra, R., Chauhan, S., et al., 2020. Metabolite profiling and wound-healing activity of Boerhavia diffusa leaf extracts using in vitro and in vivo models. J. Tradit. Complement. Med. 10 (1), 52–59.

Khamis, A.A., Ali, E.M., Abd El-Moneim, M.A., Abd-Alhaseeb, M.M., El-Magd, M.A., Salim, E.I., 2018. Hesperidin, piperine and bee venom synergistically potentiate the anticancer effect of tamoxifen against breast cancer cells. Biomed. Pharmacother. 105, 1335–1343.

Kim, S.F., Huri, D.A., Snyder, S.H., 2005. Inducible nitric oxide synthase binds, S-nitrosylates, and activates cyclooxygenase-2. Science 310 (5756), 1966–1970.

Kim, J.-G., Kim, W., Kim, K.-Y., 2023. Alpinia japonica extract induces apoptosis of hepatocellular carcinoma cells through G0/G1 cell cycle arrest and activation of JNK. Cell. Mol. Biol. 69 (2), 12–18.

Li, J., Zhou, N., Luo, K., Zhang, W., Li, X., Wu, C., Bao, J., 2014. In silico discovery of potential VEGFR-2 inhibitors from natural derivatives for anti-angiogenesis therapy. Int. J. Mol. Sci. 15 (9), 15994–16011.

Lu, X., Qian, J., Zhou, H., Gan, Q., Tang, W., Lu, J., Yuan, Y., Liu, C., 2011. In vitro cytotoxicity and induction of apoptosis by silica nanoparticles in human HepG2 hepatoma cells. Int. J. Nanomed. 1889–1901.

Lukong, K.E., 2017. Understanding breast cancer–The long and winding road. BBA Clin. 7, 64–77.

Morris, G.M., Huey, R., Lindstrom, W., Sanner, M.F., Belew, R.K., Goodsell, D.S., Olson, A.J., 2009. AutoDock4 and AutoDockTools4: Automated docking with selective receptor flexibility. J. Comput. Chem. 30 (16), 2785–2791.

Murakami, A., Ohigashi, H., 2007. Targeting NOX, INOS and COX-2 in inflammatory cells: chemoprevention using food phytochemicals. International Journal of Cancer 121 (11), 2357–2363.

Pearce, A., Haas, M., Viney, R., Pearson, S.-A., Haywood, P., Brown, C., Ward, R., 2017. Incidence and severity of self-reported chemotherapy side effects in routine care: A prospective cohort study. PLoS One 12 (10), e0184360.

Qari, S.H., Alrefaei, A.F., Filfilan, W., Qumsani, A., 2021. Exploration of the medicinal flora of the aljumum region in saudi arabia. Appl. Sci. 11 (16), 7620.

Raffoul, J.J., Kucuk, O., Sarkar, F.H., Hillman, G.G., 2012. Dietary agents in cancer chemoprevention and treatment. Journal of Oncology 2012.

Rahman, M., Ahmad, S., Mohamed, M., Ab Rahman, M., 2014. Antimicrobial compounds from leaf extracts of Jatropha curcas, Psidium guajava, and Andrographis paniculata. The Scientific World Journal 2014.

Rajeswari, G., Murugan, M., Mohan, V., 2012. GC-MS analysis of bioactive components of Hugonia mystax L. (Linaceae). Res. J. Pharm., Biol. Chem. Sci. 3 (4), 301–308.

Safarzadeh, E., Shotorbani, S.S., Baradaran, B., 2014. Herbal medicine as inducers of apoptosis in cancer treatment. Advanced Pharmaceutical Bulletin 4 (Suppl 1), 421.

Shareef, M.I., Gopinath, S., Gupta, A., Gupta, S., 2017. Antioxidant and anticancer study of Boerhavia erecta. Int. J. Curr. Microbiol. Appl. Sci 6 (9), 879–885.

Sinan, K.I., Akpulat, U., Aldahish, A.A., Celik Altunoglu, Y., Baloğlu, M.C., Zheleva-Dimitrova, D., Gevrenova, R., Lobine, D., Mahomoodally, M.F., Etienne, O.K., 2021. LC-MS/HRMS analysis, anti-enzymatic and antioxidant effects of Boerhavia diffusa extracts: a potential raw material for functional applications. Antioxidants 10 (12), 2003.

Singh, P., Alex, J.M., Bast, F., 2014. Insulin receptor (IR) and insulin-like growth factor receptor 1 (IGF-1R) signaling systems: novel treatment strategies for cancer. Med. Oncol. 31, 1–14.

Suknoppakit, P., Wangteeraprasert, A., Simanurak, O., Somran, J., Parhira, S., Pekthong, D., Srisawang, P., 2023. Calotropis gigantea stem bark extract activates HepG2 cell apoptosis through ROS and its effect on cytochrome P450. Heliyon.

Talib, W.H., Alsayed, A.R., Barakat, M., et al., 2021. Targeting drug chemo-resistance in cancer using natural products. Biomedicines. 9 (10), 1353.

R. Tammali K. Srivastava S., V Ramana, K. Targeting aldose reductase for the treatment of cancer Current cancer drug targets 11 5 2011 560 571.

Van, L.V., Pham, E.C., Nguyen, C.V., Duong, N.T.N., Le Thi, T.V., Truong, T.N., 2022. In vitro and in vivo antidiabetic activity, isolation of flavonoids, and in silico molecular docking of stem extract of Merremia tridentata (L.). Biomed. Pharmacother. 146, 112611.

Wei, L.S., Wee, W., Siong, J.Y.F., Syamsumir, D.F., 2011. of anticancer, antimicrobial, antioxidant properties and chemical compositions of Peperomia pellucida leaf extract. Acta Medica Iranica 670–674.

Xie, Z., He, B., Jiang, Z., Zhao, L., 2020. Tanshinone IIA inhibits osteosarcoma growth through modulation of AMPK-Nrf2 signaling pathway. J. Recept. Signal Transduction 40 (6), 591–598.

Xu, F., Jin, T., Zhu, Y., Dai, C., 2018. Immune checkpoint therapy in liver cancer. J. Exp. Clin. Cancer Res. 37 (1), 1–12.

Zhang, Y., Wei, R.-X., Zhu, X.-B., Cai, L., Jin, W., Hu, H., 2012. Tanshinone IIA induces apoptosis and inhibits the proliferation, migration, and invasion of the osteosarcoma MG-63 cell line in vitro. Drugs 23 (2), 212–219.